Experimental Study on Hysteresis Characteristics of the Retaining Wall of the Base-Isolated Building

Goro Miwada, Takeshi Sano & Hideo Katsumata
Obayashi Corporation, Kiyose-shi, Tokyo, Japan

Noriko Takiyama, Yoshihiro Onishi & Yasuhiro Hayashi
Kyoto University, Kyoto-shi, Kyoto, Japan

SUMMARY:
There is a possibility that base-isolated buildings will be damaged by colliding with the retaining wall during large earthquakes. For experimental validating response of the superstructure colliding with retaining wall, the experiment of the real base-isolated building colliding with the retaining wall was carried out. The analyses on the experimental results are shown below. 1) Maximum acceleration was increased and rocking vibration was induced in the superstructure by the collisions with the retaining wall. 2) By the torsional vibration of the superstructure, there is a difference between the impact time at the X1 axis and one at the X7 in the retaining wall. 3) Deformation of the retaining wall is concentrated at the points of collision and hysteresis characteristics of the retaining wall exhibit elasto-plasticity. Furthermore, analyses on experimental simulation results are shown below. 4) Simulated acceleration waveform roughly agrees with the experimental one. 5) Maximum and residual displacements of the retaining wall are overestimated.

Keywords: Base Isolation, Collision, Retaining Wall

1. INTRODUCTIONS

After the 1995 Hyogoken-Nanbu earthquake, the number of base-isolated buildings has increased in Japan. It has started to study on applying nuclear facilities to the base-isolation system in recent years. Evaluation of responses of base-isolated buildings colliding with retaining walls during large earthquakes is important because high safety is required in such facilities. Previous studies have shown earthquake response analyses of collisions with retaining walls using hysteresis characteristics of the retaining wall (e.g. Matsagar, et al., 2003). However these hysteresis characteristics which have not been validated experimentally, because there have been few experiment or observation reports until now (Kashiwa, et al., 2005 and EERI, 1996). Therefore, the experiment of the real base-isolated building colliding with retaining walls was carried out. In this paper, the analyses on the experimental results and experimental simulations are described.

2. EXPERIMENT OUTLINE

2.1. Base-isolated Building

The specification of the base-isolated building is shown in Table 2.1. The building, which is subject of the experiment, is a five story base-isolated building in Tokyo, Japan (Photo 2.1.). The superstructure of this building is a reinforced-concrete structure (RC). The elevation plans and cross section of the retaining wall of the building are shown in Figs 2.1, 2.2. The base-isolation system consists of 14 natural rubber bearings and 96 steel bar dampers. Cross section and specification of the natural bearing are shown in Fig.1.3 and Table 1.2. In this experience, these all dampers were removed. Natural period of the base-isolated building is 2.71s by the preliminary experiments (Miwada, et al., 2011).

The retaining wall is RC, 1.2 meters height, 0.2 meters thickness and 24.2 meters width. Clearance between the superstructure and the retaining wall is 375mm. In this experience, the clearance was narrowed to 25 – 32.5mm. The ground behind the retaining wall is loamy layer of the Kanto. Shear wave velocity of the ground is 143m/s. The pile of the building is prestressed high-strength (PHC) pile and is supported gravel layer.

Table 2.1. Specification of Base-Isolated Building

Site	Kiyose-shi, Tokyo, Japan
Completed	Sep., 1986
Story & Eaves Height	5 story, 21.85 m
Super Structure	RC structure
Base-isolation System	Natural Rubber Bearing: 14 bearings
	Steel Bar Damper: 96 dampers
Clearance between Super Structure and Retaining Wall	Designed: 375 mm
	Experiment: 25 – 32.5 mm

Photo 2.1. The Base-Isolated Building, which is Subject of the Experiment
Left: View of the Building, Right: Retaining Wall

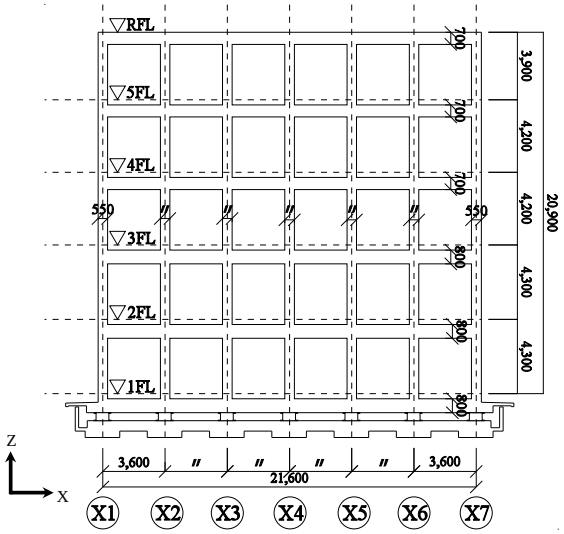

Figure 2.1. Elevation Plan of the Building

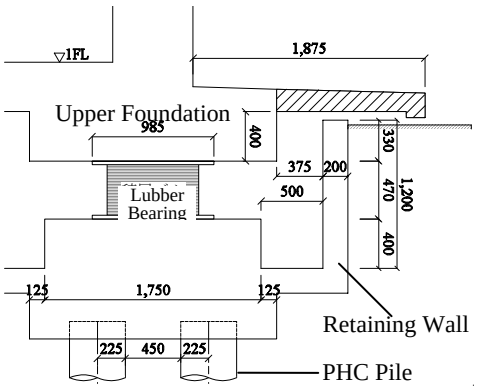

Figure 2.2. Cross Section of the Retaining Wall

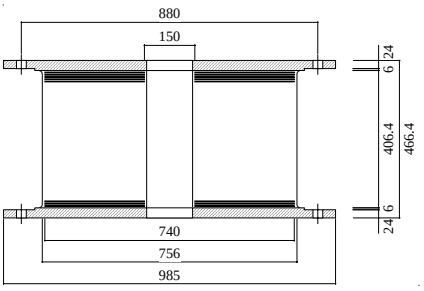

Figure 2.3. Cross Section of Rubber Bearing

Table 2.2. Specification of Natural Rubber Bearing

Diameter	Outer:740 mm, Inner:150mm
Rubber layer	4.4 mm, 61 layers
Steel plate layer	2.3mm, 60 layers
1st shape factor	33.5
2nd shape factor	2.8
Modulus of rigidity of lubber	0.55 N/mm^2
Young's modulus of lubber	1.13 N/mm^2

2.2. Experimental Method

Schematic diagram of the experimental procedure is shown in Fig 2.4. First, the base-isolated layer was statically deformed to 100mm by the jack in Y direction, and then the superstructure started free vibration by the quick-unloading of the jack, after that, collided with the retaining wall. Load cells and steel beam were set in two portion of the retaining wall and the clearance between the superstructure and the retaining wall was narrower to 25mm at the X1 axis and 32.5mm at the X7 axis. These Load cells are for measuring impact that occurs when the superstructure collides to the retaining wall. Set up the load cell on the retaining wall at the X1 axis is shown in Photo 2.2.

14 accelerometers were set in the superstructure. Accelerometers location of the base-isolated building is shown in Fig. 2.5. Displacement sensors were set in isolated layer for measuring relative displacements, and were set in clearance between the superstructure and the retaining wall for measuring displacements of the retaining wall.

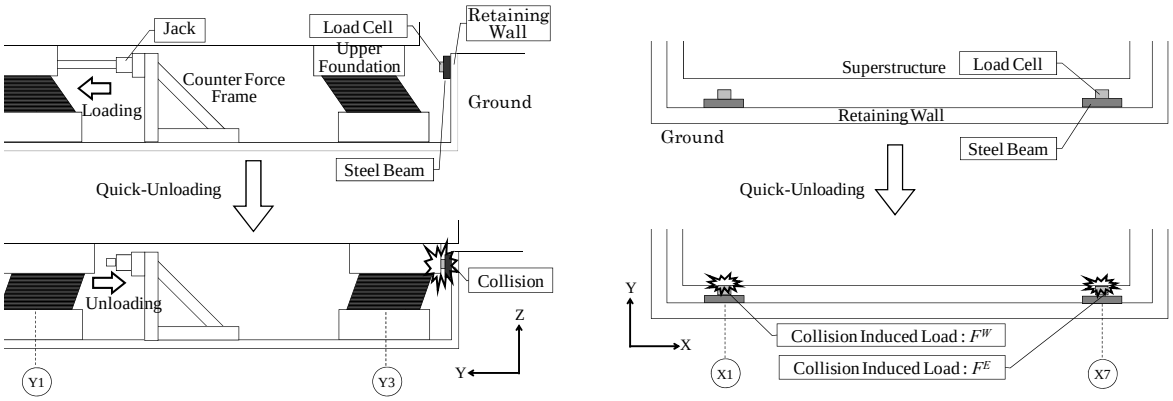

Figure 2.4. Schematic Diagram of the Experiment

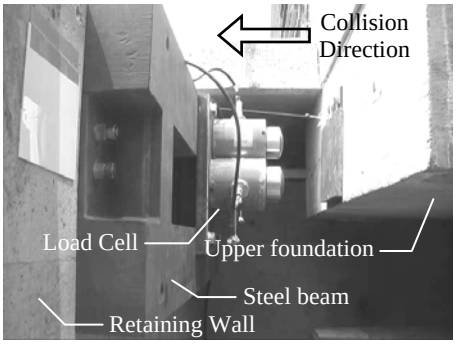

Photo 2.2. Set up the Load Cell on the Retaining Wall at the X1 Axis

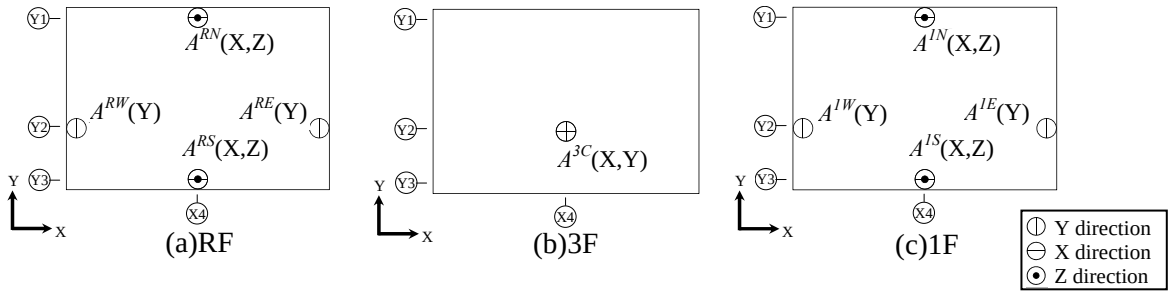

Figure 2.5. Accelerometers Location of the Base-Isolated Building

3. EXPERIMENTAL RESULT

3.1. Response in the Superstructure

Time history waveforms of response in the superstructure are shown in Fig. 3.1. The superstructure collides with the retaining wall 7 times, as shown in Fig. 3.1 (a). Relative displacement of the isolated layer is limited by collisions in negative direction, as shown in Fig. 3.1 (b). Acceleration of the superstructure at the 1st floor is increased in every impact, as shown in Fig. 3.1 (c). Maximum accelerations of the superstructure are 211cm/s^2 at A^{1W}(Y) and 206cm/s^2 at A^{1E}(Y), and is recorded at the 1st impact. Maximum accelerations at each floor are almost same.

Enlarged view of time history waveforms are shown in Fig. 3.2. There are difference of the collision time and impact load between F^W (X1 axis) and F^E (X7 axis), as shown in Fig. 3.2 (a). In addition, relative displacements of the isolated layer in X direction are opposite phase at Y1 axis and Y3 axis, as shown in Fig. 3.2 (b). Therefore, torsional vibration is induced in the superstructure. Rocking vibration is also induced in the superstructure, as shown in Fig. 3.2 (c) - (f). Rocking vibration is induced during about a second after each impact and quick-unloading. Period of rocking vibration is 0.21 seconds, as shown in Fig. 3.2 (f). Appearance natural period in time history waveforms is shorter than natural period 2.71 seconds, as the time intervals of the collisions are about 2.5 seconds, as shown in Fig. 3.2 (a) and (c).

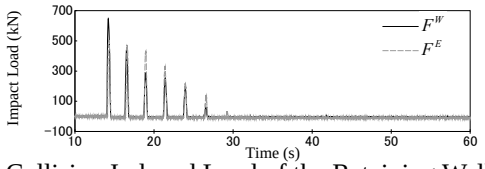

(a) Collision Induced Load of the Retaining Wall

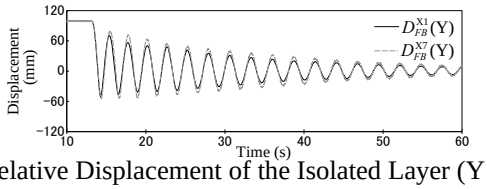

(b) Relative Displacement of the Isolated Layer (Y dir.)

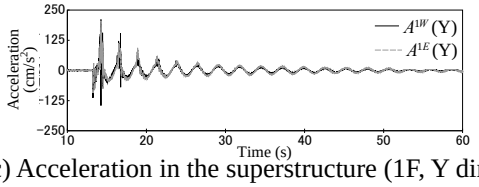

(c) Acceleration in the superstructure (1F, Y dir.)

Figure 3.1. Time History Waveforms

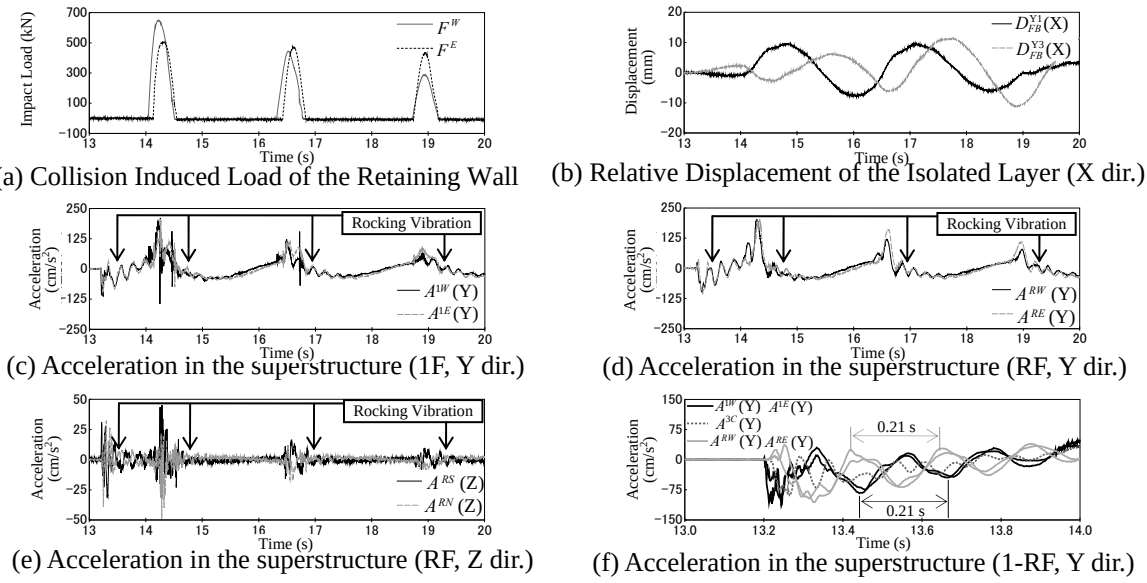

(a) Collision Induced Load of the Retaining Wall
(b) Relative Displacement of the Isolated Layer (X dir.)
(c) Acceleration in the superstructure (1F, Y dir.)
(d) Acceleration in the superstructure (RF, Y dir.)
(e) Acceleration in the superstructure (RF, Z dir.)
(f) Acceleration in the superstructure (1-RF, Y dir.)

Figure 3.2. Enlarged View of Time History Waveforms

3.2. Hysteresis Characteristics of the Retaining Wall

Hysteresis characteristics of the retaining wall are shown in Fig. 3.3. In Figs. 3.3 - 3.5, signs of displacements are inverted. Black line shows relation the load, which is sum of F^W (X1 axis) and F^E (X7 axis), and the average displacement of the retaining wall at the X1 and the X7 axis. Maximum displacements of the retaining wall without clearance are 25.4mm at the X1 axis and 21.8mm at the X7 axis. These maximum displacements are observed at height 85cm of the retaining wall. Maximum impact load is 1,150kN. The total hysteresis characteristics are represented by the bilinear model, which has primary yield load at about 500kN.

Distribution of maximum displacement of the retaining wall in the X-Y plane is shown in Fig. 3.4. Deformation of the retaining wall is concentrated in the X1 and the X7 axis where superstructure collides, as maximum displacements of measuring points 5meters away from the X1 and the X7 axis are less than 1mm.
Distribution of maximum displacement of the retaining wall in Y-Z plane is shown in Fig. 3.5. In this figure, maximum displacements at top of the retaining wall are estimated by linear interpolation. It is considered that the retaining wall became plasticity at bottom, as the retaining wall is deformed linearly in the Y-Z plane.

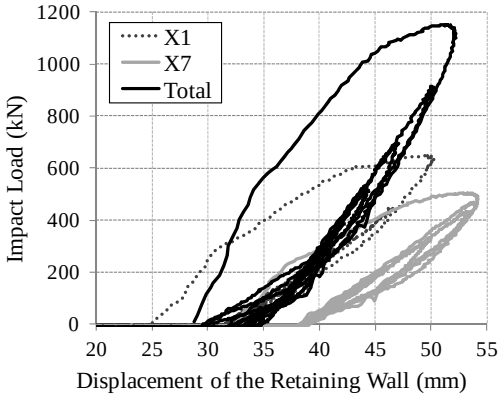

Figure 3.3. Hysteresis Characteristics of the Retaining Wall

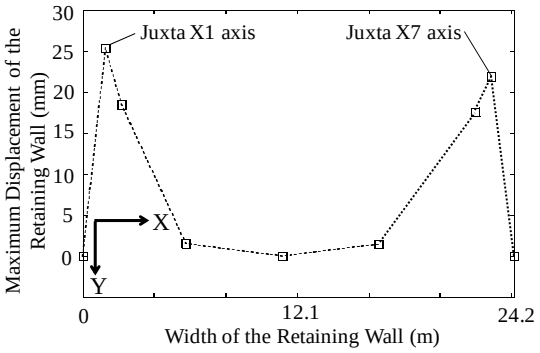

Figure 3.4. Distribution of Maximum Displacements of the Retaining Wall in the X-Y

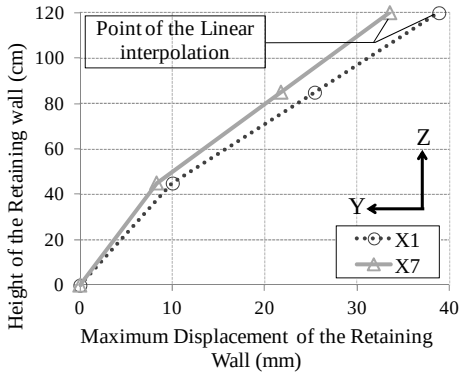

Figure 3.5. Distribution of Maximum Displacements of the Retaining Wall in the Y-Z plane

4. MODELING HYSTERESIS CHARACTERISTICS OF THE RETAINING WALL AND SIMULATION ANALYSIS

4.1. Modelling Hysteresis Characteristic of the Retaining Wall

Hysteresis characteristics of the retaining wall are modeled after experimental result. Hysteresis characteristics model of the retaining wall is shown in Fig. 4.1. In this model, primary yield load is 500kN. Primary and secondary stiffness is 104.6kN/mm and 46.4kN/mm. Schematic diagram of the retaining wall model on simulation analysis is shown in Fig. 4.2. Clearance between the superstructure and the retaining wall is 28.8mm before the retaining wall yielding and increase after that.

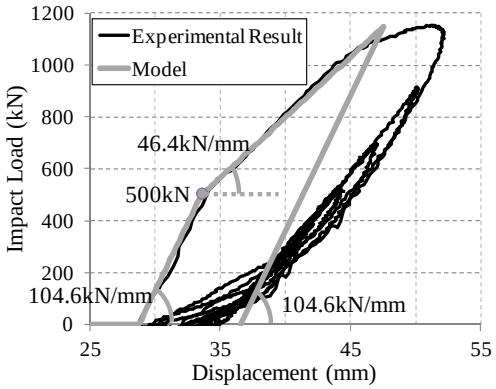

Figure 4.1. Hysteresis Characteristic Model of the Retaining Wall

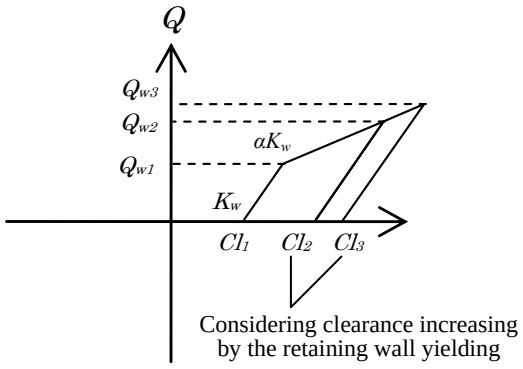

Figure 4.2. Schematic Diagram of the Retaining Wall Model on Simulation Analysis

4.2. Simulation Analysis

Simulation model of the base-isolated building and parameters are shown in Fig. 4.3 and Table 4.1. These parameters are set based on results of preliminary experiments. Rocking stiffness is estimated from the vertical stiffness of the base-isolated layer and the PHC piles. The torsional vibration is not considered in this model.

Comparison of the experimental results and simulation results in acceleration waveform is shown in Fig. 4.4. In this figure, the acceleration of the experimental result is the average of two accelerations

shown in Fig. 3.1 (c). Simulated acceleration waveform roughly agrees with experimental one. The number of the collisions in the simulation analysis is the same 7 times, which is the same as one in experimental result, as shown in Fig. 4.4 (a). At the 1st impact, maximum acceleration is underestimated by about 50cm/s^2, as shown in Fig. 4.4 (b). Comparison experimental result and simulation in relation between load and displacement is shown in Fig. 4.5. Maximum and residual displacements of the retaining wall are overestimated by 12mm and 10mm. The maximum impact load is also overestimated by 64%.

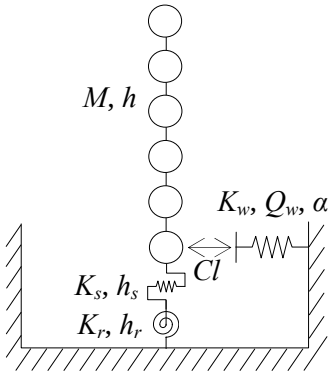

Figure 4.3. Simulation Model of the Base-Isolated Building

Table 4.1. Parameters in Simulation Analysis

Parameter		Symbol	Value
Base Isolated layer	Sway Stiffness	K_s	1.31×10^4 (kN/m)
	Damping Factor	h_s	1.8 (%)
	Rocking Stiffness	K_r	5.78×10^8 (kN・m/rad)
	Damping Factor for Rocking mode	h_r	8.0 (%)
Super Structure	Total Mass	M	2,576 (t)
	Damping Factor	h	3.0 (%)
Retaining Wall	Primary Sway Stiffness	K_w	1.05×10^5 (kN/m)
	Primary Yield Load	Q_w	500 (kN)
	Decreasing Rate of Stiffness	α	0.44
	Clearance	Cl	28.8 (mm)

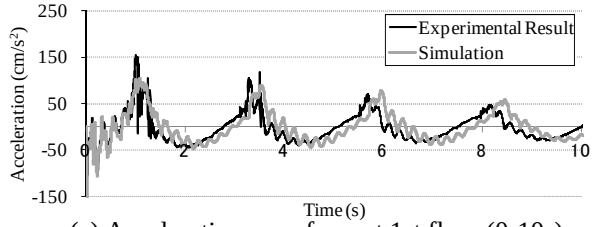

(a) Acceleration waveform at 1st floor (0-10s)

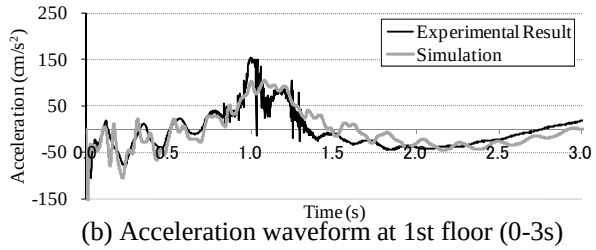

(b) Acceleration waveform at 1st floor (0-3s)

Figure 4.4. Comparison of Experimental Result and Simulation in Acceleration Waveform

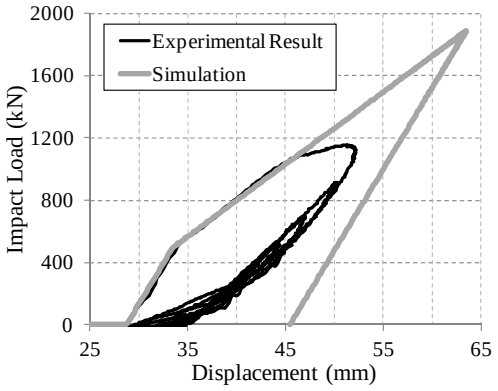

Figure 4.5. Comparison of Experimental Result and Simulation in Relation between Load and Displacement

5. CONCLUSION

In this paper, experimental results of the real base-isolated building colliding with the retaining wall have been reported. Dynamics characteristics in the base-isolated building and hysteresis characteristics of the retaining wall obtained from the observation records have been described.
The analyses on the experimental results are shown below.
1) Maximum acceleration was increased and rocking vibration was induced in the superstructure by the collisions with the retaining wall.
2) By the torsional vibration of the superstructure, there is a difference between the impact time at the X1 axis and one at the X7 in the retaining wall.

3) Deformation of the retaining wall is concentrated at the colliding points and hysteresis characteristics of the retaining wall exhibit elasto-plasticity.
Furthermore, the analyses on experimental simulation results are shown below.
4) Simulated acceleration waveform roughly agrees with experimental one.
5) Maximum and residual displacements of the retaining wall are overestimated.

REFERENCES

Matsagar, Vasant A., Jangid, R.S. (2003). Seismic response of base-Isolated structures during impact with adjacent structures. *Engineering Structures.* **25**, 1311-1323.

Kashiwa, H., Nakayasu, N., Nakashima, M. (2005). Response and Damage of Base-isolated Buildings Subjected to Very Large Earthquakes. *Architectural Institute of Japan Journal of Structural Engineering*. **51B**, 237-246. (In Japanese)

Earthquake Engineering Research Institute (EERI). (1996). Northridge earthquake of January 17 1994). Earthquake Spectra. **Vol. 2**, 243-251.

Miwada, G., Komaki, J., Sato, K., Sano, T., Katsumata, H., Takiyama, N., Hayashi. Y. (2011). Experiments and Simulation Analysis of Collision to Retaining Wall with Real Scale Base-isolated Building. *Architectural Institute of Japan Journal of Structural and Construction Engineering*. **Vol. 76:No.663**, 899-908.